

1 **Estimating~~on~~ of soil moisture water holding capacity with Random**
2 **Forests conditions for drought monitoring with Random forest and a**
3 **simple soil moisture accounting scheme**

4

5

6 Yves Tramblay ^{1*}

7 Pere Quintana Seguí ²

8

9

10 1 HydroSciences Montpellier (University Montpellier, CNRS, IRD), France

11 2 Observatori de l'Ebre (OE), Ramon Llull University – CSIC, 43520 Roquetes, Spain

12

13

14 *Corresponding author : yves.tramblay@ird.fr, 300 avenue du Pr. Emile Jeanbreau,
15 34090, Montpellier, France. +33 4 67 14 33 59

Code de champ modifié

16 **Abstract**

17

18 Soil moisture is a key variable for drought monitoring but soil moisture measurements
19 networks are very scarce. Land-surface models can provide a valuable alternative to
20 simulate soil moisture dynamics, but only a few countries have such modelling schemes
21 implemented for monitoring soil moisture at high spatial resolution. In this study, a soil
22 moisture accounting model (SMA) was regionalized over the Iberian Peninsula, taking as
23 a reference the soil moisture simulated by a high-resolution land surface model. To
24 estimate soil water holding capacity, the sole parameter required to run the SMA model,
25 two approaches were compared: the direct estimation from European soil maps using
26 pedotransfer functions, or an indirect estimation by a Machine Learning approach,
27 Random Forests, using as predictors altitude, temperature, precipitation, potential
28 evapotranspiration and land use. Results showed that the Random Forest model
29 estimates are more robust, especially for estimating low soil moisture levels.
30 Consequently, the proposed approach can provide an efficient way to simulate daily soil
31 moisture and therefore monitor soil moisture droughts, in contexts where high-resolution
32 soil maps are not available, as it relies on a set of covariates that can be reliably estimated
33 from global databases.

34

35

36

37

38

39 **Keywords:** soil moisture, droughts, random forests

40

41

42 1. Introduction

43

44 Soil moisture droughts have strong impacts on vegetation and agricultural production
45 (Raymond et al., 2019; Tramblay et al., 2020; Vicente-Serrano et al., 2014; Pena-Gallardo
46 et al., 2019). There is a growing interest for simple indicators to monitor drought events
47 at short timescales that could be related to impacts (Li et al., 2020; Noguera et al., 2021).
48 In particular, soil moisture indicators could be more relevant than climatic ones to monitor
49 potential impacts of droughts on agriculture and natural vegetation (Piedallu et al., 2013).
50 Since actual soil moisture measurements remain very scarce, soil moisture simulated
51 from land-surface models are an interesting proxy to develop simplified methodologies
52 that could be applied on data-sparse regions. Land-surface models (LSM) are valuable
53 tools for a fine scale monitoring of drought events; however, their implementation requires
54 accurate forcing data and computational resources (Almendra-Martín et al., 2021;
55 Quintana-Seguí et al., 2019; Barella-Ortiz and Quintana-Seguí, 2019). Global
56 implementation also exists but with a coarser resolution and driven by reanalysis data
57 (Rodell et al., 2004; Muñoz Sabater, 2020) that may not be adequate for local-scale
58 applications. Only very few countries have land-surface schemes implemented at the
59 national level to monitor droughts (Habets et al., 2008).

60

61 Remote Sensing is another option which allows monitoring soil moisture (Dorigo et al.,
62 2017; Brocca et al., 2019). Microwave sensors allow monitoring of surface soil moisture
63 (first 5 cm for L-band based products, skin for C-band based products), without the
64 interference of clouds. However, surface soil moisture is not enough for most applications,
65 which require root zone soil moisture, which is the water resource in the soil available to
66 plants. Furthermore, passive L-band products, such as SMOS (Martínez-Fernández et
67 al., 2016) or SMAP (Mishra et al., 2017), have a low resolution and active C-band
68 products, such as Sentinel 1 (Bauer-Marschallinger et al., 2019), which have higher
69 resolution, suffer from higher noise and are more sensitive to vegetation. Thus, even
70 though remote sensing is very useful, it still has problems to be surmounted. The
71 resolution of passive L-band products can be increased using optical data (NDVI, LST),
72 by means of downscaling algorithms (Merlin et al., 2013; Fang et al., 2021), but then the
73 resulting product is sensitive to cloud cover. Also, some progress has been made in
74 deriving root zone soil moisture from surface soil moisture estimations using an
75 exponential filter (Stefan et al., 2021) calibrated using the SURFEX LSM (Masson et al.,
76 2013), but these products are in early stages and are not operational yet.

77

78 Simplified methodologies to estimate and monitor the status of soil moisture, are needed
79 in contexts where LSM data is not available and where remote sensing products fall short,
80 such as areas and time periods with dense vegetation, or high soil roughness which may

81 affect their accuracy (Escorihuela and Quintana-Seguí, 2016). Different modelling
82 approaches have been proposed, either with conceptual soil moisture accounting models
83 or computational variants of the antecedent precipitation index (Willgoose and Perera,
84 2001; Javelle et al., 2010; Brocca et al., 2014; Zhao et al., 2019; Li et al., 2020). The
85 general availability of spatial estimates of soil moisture content would help introduce soil
86 moisture in drought monitoring systems, improving their scope and usefulness.
87 Furthermore, this would also facilitate the creation of long-term reanalysis, based on
88 meteorological forcing data, and future climate change studies, without the need of
89 running LSM models. However, to apply this type of models at regional or national scale,
90 there is a need to estimate their parameters over the area of interest. For that purpose,
91 regionalization methods have been employed in hydrology for decades to estimate the
92 parameters of hydrological models in ungauged basins (Blöschl and Sivapalan, 1995; He
93 et al., 2011; Hrachowitz et al., 2013). Several methods exist, based either on catchment
94 similarity or the direct estimation of model parameters using regression techniques with
95 physiographic attributes. For soil moisture modelling, up to now only very few studies
96 have considered these approaches to apply soil moisture accounting models at ungauged
97 locations (Grillakis et al., 2021) or estimate root zone soil moisture using machine learning
98 methods (Carranza et al., 2021).

99
100 The goal of the present study is to regionalize a simple soil moisture accounting (SMA)
101 scheme that could be used to monitor soil moisture droughts. The SMA model considered
102 in the present study requires a single parameter, the maximum soil water holding
103 capacity. Two different approaches are compared to estimate this parameter regionally:
104 the direct estimation with soil maps or with a machine learning technique, namely
105 Random Forests.

106
107 **2. Study area and Data**
108
109 The study area of this work is the Iberian Peninsula, which is located between the
110 Mediterranean Sea and the Atlantic Ocean and thus is influenced by both synoptic scale
111 systems, that often come from the Atlantic side, and mesoscale heavy precipitation
112 events, that often come from the Mediterranean side. The Iberian Peninsula presents a
113 marked relief, with a large and high central plateau and different mountain ranges, which
114 heavily influence the spatial patterns of precipitation, enhancing it windward and
115 decreasing it leeward, generating areas of high precipitation on the west, north-west and
116 north, and very dry areas on the central plains and, specially, on the South-east, as a
117 consequence the Iberian Peninsula has a heterogeneous distribution of average annual
118 rainfall, with values ranging from 2000 mm/y to less than 100 mm/y. All this has a strong
119 influence on the spatial and temporal variability of soil moisture and soil moisture regimes,
120 having wet regimes on the west and north, where the soil is hardly stressed and, and

121 semi-arid areas elsewhere, with a wet (energy limited) and a dry (water limited) season,
122 with a dry down that might be interrupted by convective events. All this makes the
123 modelling of soil moisture in Iberian a rather challenging task.

124
125 Daily precipitation, temperature and potential evapotranspiration (PET) were retrieved
126 from the SAFRAN-Spain database (Quintana-Seguí et al., 2017). SAFRAN (Durand et
127 al., 1993) is a meteorological reanalysis that produces gridded datasets by combining the
128 outputs of a meteorological model and all available observations using an optimal
129 interpolation algorithm. It has been implemented over France (Quintana-Seguí et al.,
130 2008) and recently over the Iberian Peninsula (Quintana-Seguí et al., 2017) with a
131 5kmx5km spatial resolution. The SAFRAN dataset used in this study not only includes
132 observations from the Spanish part of the Iberian Peninsula, it has also ingested data
133 from Portugal. The SURFEX LSM (Masson et al., 2013) has been run using SAFRAN-
134 Spain as the meteorological forcing dataset and on the same grid, as it was done in
135 Quintana-Seguí et al., (2020~~2019~~). SURFEX uses the ECOCLIMAP2 (Faroux et al.,
136 2013) physiographic database and it uses the ISBA (Interaction Sol-Biosphère-
137 Atmosphère) scheme (Noilhan and Mahfouf, 1996) for natural surfaces. ISBA has
138 different options; we have used ISBA-DIF, the multi-layer diffusion version (Boone 2000;
139 Habets et al. 2003). From this simulation, we have extracted the soil moisture of the first
140 60 cm of the soil, by performing the weighted average of the soil layers that fall within this
141 range. This simulated soil moisture over the Iberian Peninsula is considered herein as the
142 observed reference, in the absence of dense monitoring networks of soil moisture
143 (Martínez-Fernández et al., 2014~~2016~~). From the ECOCLIMAP2 database, elevation and
144 land cover data have also been retrieved and aggregated in the following nine categories:
145 water, bare, ice/snow, urban, forest, grass, dry crops, irrigated crops, wetlands.

146
147 We also use the European Soil database (ESDB) produced by the European Soil Data
148 Centre (Panagos et al., 2012). The ESDB contains information on soil characteristics,
149 including soil depth and texture for topsoil (0-30cm) and subsoil (30-70cm) layers at a
150 grid resolution of 1 km. The total available water content (TAWC) is a volumetric
151 parameter describing the water content between field capacity and permanent wilting
152 point, as a function of available water content, presence of coarse fragments and depth
153 (Reynolds et al., 2000). In ESDB, water content at field capacity and permanent wilting
154 point were determined following the equation from (van Genuchten, 1980) to estimate the
155 soil water retention curve (Hiederer, 2013). The parameters of the equation are provided
156 by a pedotransfer function (Wösten et al., 1999) for volumetric soil water content
157 computed from the soil water retention curve. The pedotransfer function uses soil texture,
158 organic carbon content and bulk density to determine the parameters of the soil water
159 retention curve (Hiederer, 2013).
160

161 **3. Methods**

162

163 **3.1 Soil moisture accounting model**

164

165 The soil moisture model considered here has been previously applied in several studies
 166 for applications related to soil moisture monitoring (Anctil et al., 2004; Javelle et al., 2010;
 167 Tramblay et al., 2012, 2014), it consists in the SMA part of the GR4J model (Perrin et al.,
 168 2003), driven by precipitation and PET, that represents a conceptual formulation of the
 169 impact of precipitation and PET on soil water balance, using a soil reservoir of fixed depth,
 170 A. This parameter represents the maximum capacity of that reservoir, that can be
 171 assumed to be equivalent to the soil water holding capacity (Perrin et al., 2003, Javelle
 172 et al., 2010, Tramblay et al., 2014). The soil reservoir has either a net outflow when PET
 173 exceed rainfall:

174

175

176 If $P_t \leq PET_t$

177
$$S^* = S_{t-1} - \frac{S_{t-1}(2A - S_{t-1}) \tanh\left(\frac{PET_t - P_t}{A}\right)}{A + (A - S_{t-1}) \tanh\left(\frac{PET_t - P_t}{A}\right)} \quad (1)$$

178

179 Or net inflow in all the other cases:

180

181 If $P_t \geq PET_t$

182
$$S^* = S_{t-1} + \frac{(A^2 - S_{t-1}^2) \tanh\left(\frac{P_t - PET_t}{A}\right)}{(A + S_{t-1}) \tanh\left(\frac{P_t - PET_t}{A}\right)} \quad (2)$$

183

184 Where S^* can never exceed the maximum reservoir capacity. Finally, the outflow from
 185 the storage reservoir due to percolation is taken into account using:

186

187
$$S_t = S^* \left[1 + \left(\frac{4S^*}{9A} \right)^4 \right]^{-\frac{1}{4}} \quad (3)$$

a mis en forme : Police :12 pt

188

189 The level of the soil reservoir is given by S/A, ranging between 0 and 1, which provides a
190 soil wetness index (SWI) for the catchment. The outputs of SURFEX soil moisture are
191 first normalized with the maximum and minimum values, to obtain a SWI consistent with
192 the SMA model output. Then, the SMA model parameter A is calibrated using this
193 normalized SURFEX soil moisture as a reference. The SMA model is calibrated for each
194 grid cell independently using soil moisture simulated with SURFEX covering the full
195 Iberian Peninsula domain. The Nelder-Mead simplex algorithm is used for the calibration
196 with the Nash efficiency criterion. To regionally estimate the values of A, two different
197 methods are compared: the direct estimation of A with TAWC from ESDB soil maps or its
198 indirect estimation with machine learning methods, namely Random Forests using
199 5kmx5km grid physiographic and climatic properties.

200

201 **3.2 Regionalization with soil maps**

202
203 The first approach consists in using the total available water content from the ESDB
204 database to estimate the A parameter for each grid cell. In the present work, the TAWC
205 of subsoil and topsoil layers have been added and averaged at the scale of 5km x 5km,
206 matching the spatial resolution of the SAFRAN grid. Then, these estimates have been
207 used to set the A parameter of the SMA model. Thus, this regionalization approach is
208 based on the a priori estimation of the A parameter from soil maps solely.

209

210 **3.2-3 Regionalization with Random forests**

211

212 Random Forests (Breiman, 2001) belong to the class of Machine Learning techniques.
213 RF are based on a bootstrap aggregation (Breiman, 1996) of Classification and
214 Regression Trees (Breiman et al., 2017). It generates a bootstrap sample from the original
215 data and trains a tree model using this sample. The procedure is repeated many times
216 and the bagging's prediction is the average of the predictions. Among the many
217 advantages of RF, they are fast, non-parametric, robust to noise in the predictor variables,
218 able to capture nonlinear dependencies between predictors and dependent variables and
219 they can simultaneously incorporate continuous and categorical variables (Tyralis et al.,
220 2019). The drawbacks are they are complex to interpret and they cannot extrapolate
221 outside the training range. Given their advantages, this algorithm is particularly suited for
222 the estimation of spatial variables such as soil properties (Booker and Woods, 2014;
223 Hengl et al., 2018; Gagkas and Lilly, 2019; Stein et al., 2021). In the present work, a RF
224 model is generated to estimate the values of the A parameter of the SMA model,
225 representing soil water holding capacity, with the properties of the 5x5km grid cells namely
226 altitude, land cover, mean annual precipitation, temperature and PET, using Random Forests.

228 To estimate the reliability of the method, the 5km x 5km grid cells covering the Iberian
229 Peninsula have been split randomly into a training sample containing 70% of the cells
230 ([15636 data points](#)) and a testing sample with the 30% remaining cells ([6701 data points](#)).
231 The random selection of the training and testing sets have been performed using a Latin
232 Hypercube Sampling (McKay et al., 1979) to ensure a homogeneous sampling over the
233 Iberian Peninsula. Given that the RF trees cannot be interpreted directly, as for example
234 the weights in a linear regression, we additionally implemented an out-of-bag predictor
235 importance estimation by permutation (Loh and Shih, 1997), to measure how influential
236 the predictor variables in the model are at predicting the response. The influence of a
237 predictor increases with the value of this measure. If a predictor is influential in prediction,
238 then permuting its values should affect the model error. If a predictor is not influential,
239 then permuting its values should have little to no effect on the model error.
240

241 **3.3 Validation on the ability to detect dry soil moisture conditions**

242
243 To compare the efficiency of the two methods compared to estimate the A parameter of
244 the SMA model, the SMA model was run using the two methods and all daily values of
245 soil moisture below the 10th percentile were extracted, corresponding to dry soil
246 conditions. Only the grid cells in the testing sample were considered for this validation.
247 We computed different verification scores to assess the relative efficiency of the two
248 methods to reproduce daily soil moisture below the 10th percentile using the ISBA
249 simulated soil moisture as a benchmark; the Probability of Detection (POD), the False
250 Alarm Ratio (FAR) and the Heidke Skill Score (HSS) summarizing the global efficiency to
251 detect dry periods (Jolliffe and Stephenson, 2011). These scores are based on the
252 contingency table between forecasts (or simulated values in the case of the present
253 study) and observations (Table 1).
254

255 POD is the probability of detection (equation 1), FAR is the number of false alarms per
256 the total number of warnings or alarms (equation 2) and HSS is a skill score ranging from
257 $-\infty$ to 1 (equation 3), for categorical forecasts where the proportion of correct measure is
258 scaled with the reference value from correct forecasts due to chance.
259

260 $POD = a / (a + c)$ [eq.1\(4\)](#)

261 $FAR = b / (a + b)$ [eq.2\(5\)](#)

262 $HSS = 2(ad - bc) / (a + b)(b + d) + (a + c)(c + d)$ [eq.3\(6\)](#)

263 **4. Results**

268

269 **4.1 Calibration of the SMA model**

270

271 The calibration results of the SMA model against SURFEX soil moisture provide very
 272 good model performance, with a mean Nash coefficient equal to 0.94, indicating its ability
 273 to reproduce the soil moisture dynamics as simulated by SURFEX. Nash values below
 274 0.5 are found for 1.21 % of grid cells (n= 273), only for areas located in the mountainous
 275 range affected by snow processes, above 1500 m.a.s.l. (Figure 1). This outcome is
 276 expected, since the SMA model does not include a snow-module it cannot reproduce
 277 snow dynamics in these areas. However, high-elevation areas with seasonal snow cover
 278 are not the area's most at risk of soil moisture droughts for agricultural activities in Spain.
 279 The calibrated values of the A parameter of the SMA model ranges from 60 to 250 mm,
 280 depending on the location (Figure 3). There is no significant correlation between A and
 281 mean annual precipitation or the aridity index (P/PET). This highlights the interplays
 282 between soil properties and climate to explain the spatial variability on soil water holding
 283 capacity.

284

285 **4.2 Regional estimation of the A parameter**

286

287 The values of the calibrated A parameter are related to the properties of the 5x5km grid
 288 cells using Random Forests. First, an out-of-bag predictor importance estimation by
 289 permutation is applied to compute the overall performance of RF and estimate the relative
 290 influence of each predictor. When using the A out-of-bag estimates in-cross-validation to
 291 run the SMA model, the loss of performance is very small, the decrease in Nash values
 292 in validation is on average equal -0.0019 (with a maximum decrease of -0.04). This is
 293 due to the small sensitivity of the SMA model to the value of A, given that the error in the
 294 estimation of A is in the range of 10 mm (RMSE = 13.18 mm). This type of validation
 295 mimics the case when the estimation at one single location is required, yet since all the
 296 remaining points are used for the estimation, it makes the approach in that case very
 297 robust. The relative importance for each predictor is plotted on Figure 3, indicating that
 298 precipitation and potential evapotranspiration are two most important predictors, followed
 299 by altitude. On the contrary, the land cover attributes for each grid cell are the least
 300 important predictors, and removing them from the RF model does not significantly change
 301 the results. This shows shows the relative importance of climatic variables in the spatial
 302 variability of soil moisture holding capacity.

303

304 To estimate the robustness of the method, we applied a split-sample validation into a
 305 testing and a training sample. 70% of the grid cells (15636 data points) were selected for
 306 training the RF model, and the remaining 30% (6701 data points) for testing. The results
 307 are presented for the testing set (Figure 4). The performance in terms of Nash for the

308 SMA model with A estimated by Random Forests or soil map is very similar, with mean
309 Nash equal to 0.86 (median = 0.89) with RF and 0.81 (median = 0.85) with soil maps. The
310 Nash values in validation (testing set) are low, or even negative, only for mountainous
311 ranges, as expected. Overall, the spatial patterns of the Nash coefficients obtained with
312 RF or ESDB are very similar too. There are no significant relationships between model
313 efficiency and the aridity index or the presence of irrigated areas, as identified in the
314 ECOCLIMAP2 land cover database.

315
316 **4.3 Estimation of dry soil conditions**
317
318 A further validation is made for daily soil moisture below the 10th percentile corresponding
319 to dry soil conditions. We computed the Probability of Detection (POD), the False Alarm
320 Ratio (FAR) and the Heidke Skill Score (HSS) summarizing the global efficiency to detect
321 dry periods. For both approaches to estimate A, the mean POD is very high, close to
322 97%, while the FAR is close to 3%. But these average results hide some discrepancy in
323 the different regions (Figure 5 [and 6](#)): the efficiency is the highest for the North-Western
324 region, the wettest areas of Spain, [with the most important increase of HSS and POD,](#)
325 [associated with a decrease in FAR, using Random forests,](#) while in the South and Central
326 parts of Spain the performance is lower on average [and very similar with the two](#)
327 [regionalization approaches.](#) For the wettest parts of the Iberian Peninsula, the POD
328 remains higher than 94% and the FAR lower than 6% and it is the region where the main
329 improvements with RF are observed. [As shown in Figure 5, the results with Random](#)
330 [forests mostly follow the climate conditions, with improved estimations in the wettest](#)
331 [regions of North and Northwestern part of Spain. For the estimation with EU soil maps,](#)
332 [the results seem related to soil depth and to a lesser extent, land cover. Indeed, higher](#)
333 [scores are found in regions with shallow soils, such as those of plutonic \(Galician region,](#)
334 [western parts of the Extremaduran mountainous ranges, Douro basin\) or metamorphic](#)
335 [origins \(western Cantabrian range, north Iberian range, eastern-central regions and Sierra](#)
336 [Morena in Andalucia\) and also sedimentary regions with shallow limestones \(eastern](#)
337 [Cantabrian mountains, Basque region, Southern Iberian range\). On the opposite, lower](#)
338 [scores are found in regions with the deepest soils \(Guadalquivir floodplains, Mid- Tagus](#)
339 [River, upper Duero, piedmonts of Cantabrian in Leon and Palencia, most of Middle](#)
340 [Navarra\). With the exception of regions such as Biscaya or coastal Portugal, with a dense](#)
341 [forest cover \(mostly Pinus radiata or pinaster\) where soil depth is probably overestimated.](#)
342 On average, the RF estimation method outperforms the approach based on ESDB (Figure
343 7), with more stable results in terms of HSS since all values obtained with RF are above
344 0.4 while with ESDB for the grid cells the HSS scores drops to values close to zero.

345
346 **5. Summary and conclusions**
347

348 In this study, a simple model allowing the monitoring of ~~the~~ soil moisture conditions
349 saturation level was regionalized over the entire Iberian Peninsula, taking as a reference
350 the soil moisture simulated by a high-resolution land surface model. Two different
351 regionalization methods have been compared, either the direct estimation of soil water
352 holding capacity from European soil maps or by Random Forests, using covariates such
353 as altitude, temperature, precipitation, potential evapotranspiration and land cover.
354 Results have shown that the estimation by Random Forest is more robust notably to
355 estimate low soil moisture levels. Despite similar average performance between the two
356 methods, the use of soil maps to set the water holding capacity reveals less stable results
357 in some cases, most probably related to the uncertainties in the pedo-transfer functions
358 used. While these pedo-transfer functions are process-based predictive functions of
359 certain soil properties, Random Forest are not based on physical processes and are
360 tailored to provide the best estimates in a statistical sense. Therefore, they provide a
361 valuable alternative in contexts where high-resolution soil maps are not available since
362 they rely on a set of covariates that can be reliably estimated from global databases, such
363 as satellite or reanalysis products (Funk et al., 2015; Hersbach et al., 2020; Muñoz
364 Sabater, 2020).

365
366 It should be noted that the results presented herein are highly dependent on the quality
367 of land surface simulations, in the absence of dense monitoring networks of in situ soil
368 moisture data, thus these results suffer from the same limitations as LSMs, notably, the
369 lack of human processes (irrigation). However, new remote sensing irrigation estimates
370 are being developed (Massari et al., 2021), as a consequence, once the RF model is
371 trained, irrigation estimations could be added to the precipitation forcing data in order to
372 include the human impacts on soil moisture estimations. The results show that this
373 approach allows us to cheaply extend the value of high resolution LSM simulations to
374 areas where no LSM is implemented (ie. north Africa), as long as the climate conditions
375 belong to the range of values used to train the model, mostly in terms of precipitation and
376 potential evapotranspiration ranges. Thus, the model train over the Iberian Peninsula
377 could be applied to other similar areas such as North Africa, Italy or Greece. As a
378 perspective, other simulations from countries where high resolution LSM simulations are
379 available, such as France or the USA, could be added to the database in order to expand
380 the coverage over different physiographic and climate contexts (Ma et al., 2021).
381 Consequently, the benefits of LSM simulations of soil moisture could be expanded to
382 other areas, provided that suitable forcing datasets are available. Furthermore, if public
383 meteorological and hydrological organizations were to create soil moisture observation
384 networks, cleverly designed to cover the most relevant climates of their countries, this
385 approach could be used to train the model using these observations and then regionalize
386 the results to the rest of the territory, thus, converting an *in-situ* observation dataset into
387 a gridded dataset with a much greater spatial coverage.

388
389

390 **Acknowledgements**

391 This work is a contribution to the HyMeX programme through the HUMID [project](#)
392 (CGL2017-85687-R, AEI/FEDER, UE) [and ANR HILIAISE projects](#). [We thank Jaime](#)
393 [Gaona \(Instituto de Investigación en agrobiotecnología CIALE, Universidad de Salamanca,](#)
394 [Villamayor, Salamanca, Spain\) for his comments on some aspects of the manuscript, and two](#)
395 [anonymous reviewers for their suggestions to improve the manuscript.](#)

396

397

398

399

400

401

402

403

404

405 **References**

a mis en forme : Anglais (États-Unis)

406
407 Almendra-Martín, L., Martínez-Fernández, J., González-Zamora, Á., Benito-Verdugo, P., and
408 Herrero-Jiménez, C. M.: Agricultural Drought Trends on the Iberian Peninsula: An Analysis
409 Using Modeled and Reanalysis Soil Moisture Products, *Atmosphere*, 12, 236,
410 <https://doi.org/10.3390/atmos12020236>, 2021.

411
412 Anctil, F., Michel, C., Perrin, C., and Andréassian, V.: A soil moisture index as an auxiliary ANN
413 input for stream flow forecasting, *Journal of Hydrology*, 286, 155–167,
414 <https://doi.org/10.1016/j.jhydrol.2003.09.006>, 2004.

415
416 Barella-Ortiz, A. and Quintana-Seguí, P.: Evaluation of drought representation and propagation
417 in regional climate model simulations across Spain, *Hydrol. Earth Syst. Sci.*, 23, 5111–5131,
418 <https://doi.org/10.5194/hess-23-5111-2019>, 2019.

419
420 Bauer-Marschallinger, B., Freeman, V., Cao, S., Paulik, C., Schaufler, S., Stachl, T., Modanesi,
421 S., Massari, C., Ciabatta, L., Brocca, L., and Wagner, W.: Toward Global Soil Moisture
422 Monitoring With Sentinel-1: Harnessing Assets and Overcoming Obstacles, *IEEE Trans.*
423 *Geosci. Remote Sensing*, 57, 520–539, <https://doi.org/10.1109/TGRS.2018.2858004>, 2019.

424
425 Blöschl, G. and Sivapalan, M.: Scale issues in hydrological modelling: A review, *Hydrol.*
426 *Process.*, 9, 251–290, <https://doi.org/10.1002/hyp.3360090305>, 1995.

427
428 Booker, D. J. and Woods, R. A.: Comparing and combining physically-based and empirically-
429 based approaches for estimating the hydrology of ungauged catchments, *Journal of Hydrology*,
430 508, 227–239, <https://doi.org/10.1016/j.jhydrol.2013.11.007>, 2014.

431
432 Boone, A., :Modélisation des processus hydrologiques dans le schéma de surface ISBA:
433 Inclusion d'un réservoir hydrologique, du gel et modélisation de la neige. [PhD thesis](#), Université

a mis en forme : Anglais (États-Unis)

434 Paul Sabatier (Toulouse III), <http://www.cnrm.meteo.fr/IMG/pdf/boone thesis 2000.pdf>, 2000.

435

436 Breiman, L.: Bagging predictors, *Mach Learn*, 24, 123–140,
437 https://doi.org/10.1007/BF00058655, 1996.

438

439 Breiman, L.: Random Forests, 45, 5–32, https://doi.org/10.1023/A:1010933404324, 2001.

440

441 Breiman, L., Friedman, J. H., Olshen, R. A., and Stone, C. J.: *Classification And Regression*
442 *Trees*, 1st ed., Routledge, https://doi.org/10.1201/9781315139470, 2017.

443

444 Brocca, L., Camici, S., Melone, F., Moramarco, T., Martínez-Fernández, J., Didon-Lescot, J.-F.,
445 and Morbidelli, R.: Improving the representation of soil moisture by using a semi-analytical
446 infiltration model, *Hydrol. Process.*, 28, 2103–2115, https://doi.org/10.1002/hyp.9766, 2014.

447

448 Brocca, L., Filippucci, P., Hahn, S., Ciabatta, L., Massari, C., Camici, S., Schüller, L., Bojkov, B.,
449 and Wagner, W.: SM2RAIN–ASCAT (2007–2018): global daily satellite rainfall data from
450 ASCAT soil moisture observations, *Earth Syst. Sci. Data*, 11, 1583–1601,
451 https://doi.org/10.5194/essd-11-1583-2019, 2019.

452

453 Carranza, C., Nolet, C., Pezij, M., and van der Ploeg, M.: Root zone soil moisture estimation
454 with Random Forest, *Journal of Hydrology*, 593, 125840,
455 https://doi.org/10.1016/j.jhydrol.2020.125840, 2021.

456

457 Dorigo, W., Wagner, W., Albergel, C., Albrecht, F., Balsamo, G., Brocca, L., Chung, D., Ertl, M.,
458 Forkel, M., Gruber, A., Haas, E., Hamer, P. D., Hirschi, M., Ikonen, J., de Jeu, R., Kidd, R.,
459 Lahoz, W., Liu, Y. Y., Miralles, D., Mistelbauer, T., Nicolai-Shaw, N., Parinussa, R., Pratola, C.,
460 Reimer, C., van der Schalie, R., Seneviratne, S. I., Smolander, T., and Lecomte, P.: ESA CCI
461 Soil Moisture for improved Earth system understanding: State-of the art and future directions,
462 *Remote Sensing of Environment*, 203, 185–215, https://doi.org/10.1016/j.rse.2017.07.001,
463 2017.

464

465 Durand, Y., Brun, E., Merindol, L., Guyomarc'h, G., Lesaffre, B., and Martin, E.: A
466 meteorological estimation of relevant parameters for snow models, *A. Glaciology.*, 18, 65–71,
467 https://doi.org/10.1017/S026030550011277, 1993.

468

469 Escorihuela, M. J. and Quintana-Seguí, P.: Comparison of remote sensing and simulated soil
470 moisture datasets in Mediterranean landscapes, *Remote Sensing of Environment*, 180, 99–114,
471 https://doi.org/10.1016/j.rse.2016.02.046, 2016.

472

473 Fang, B., Kansara, P., Dandridge, C., and Lakshmi, V.: Drought monitoring using high spatial
474 resolution soil moisture data over Australia in 2015–2019, *Journal of Hydrology*, 594, 125960,
475 https://doi.org/10.1016/j.jhydrol.2021.125960, 2021.

476

477 Faroux, S., Kaptué Tchuenté, A. T., Roujean, J.-L., Masson, V., Martin, E., and Le Moigne, P.:
478 ECOCLIMAP-II/Europe: a twofold database of ecosystems and surface parameters at 1 km
479 resolution based on satellite information for use in land surface, meteorological and climate
480 models, *Geosci. Model Dev.*, 6, 563–582, https://doi.org/10.5194/gmd-6-563-2013, 2013.

481

482 Funk, C., Peterson, P., Landsfeld, M., Pedreros, D., Verdin, J., Shukla, S., Husak, G., Rowland,
483 J., Harrison, L., Hoell, A., and Michaelsen, J.: The climate hazards infrared precipitation with

a mis en forme : Anglais (États-Unis)

a mis en forme : Anglais (États-Unis)

484 stations—a new environmental record for monitoring extremes, *Sci Data*, 2, 150066,
485 <https://doi.org/10.1038/sdata.2015.66>, 2015.

486

487 Gagkas, Z. and Lilly, A.: Downscaling soil hydrological mapping used to predict catchment
488 hydrological response with random forests, *Geoderma*, 341, 216–235,
489 <https://doi.org/10.1016/j.geoderma.2019.01.048>, 2019.

490

491 van Genuchten, M. Th.: A Closed-form Equation for Predicting the Hydraulic Conductivity of
492 Unsaturated Soils, *Soil Science Society of America Journal*, 44, 892–898,
493 <https://doi.org/10.2136/sssaj1980.03615995004400050002x>, 1980.

494

495 Grillakis, M. G., Koutoulis, A. G., Alexakis, D. D., Polykretis, C., and Daliakopoulos, I. N.:
496 Regionalizing Root-Zone Soil Moisture Estimates From ESA CCI Soil Water Index Using
497 Machine Learning and Information on Soil, Vegetation, and Climate, *Water Res*, 57,
498 <https://doi.org/10.1029/2020WR029249>, 2021.

499

500 Habets F., Boone A., and Noilhan J.: Simulation of a Scandinavian basin using the diffusion
501 transfer version of ISBA. *Glob Planet Chang* 38(1-2):137–149, 2003.

502

503 Habets, F., Boone, A., Champeaux, J. L., Etchevers, P., Franchistéguy, L., Leblois, E., Ledoux,
504 E., Le Moigne, P., Martin, E., Morel, S., Noilhan, J., Quintana Seguí, P., Rousset-Regimbeau,
505 F., and Viennot, P.: The SAFRAN-ISBA-MODCOU hydrometeorological model applied over
506 France, *J. Geophys. Res.*, 113, D06113, <https://doi.org/10.1029/2007JD008548>, 2008.

507

508 He, Y., Bárdossy, A., and Zehe, E.: A review of regionalisation for continuous streamflow
509 simulation, *Hydrol. Earth Syst. Sci.*, 15, 3539–3553, <https://doi.org/10.5194/hess-15-3539-2011>,
510 2011.

511

512 Hengl, T., Nussbaum, M., Wright, M. N., Heuvelink, G. B. M., and Gräler, B.: Random forest as
513 a generic framework for predictive modeling of spatial and spatio-temporal variables, 6, e5518,
514 <https://doi.org/10.7717/peerj.5518>, 2018.

515

516 Hersbach, H., Bell, B., Berrisford, P., Hirahara, S., Horányi, A., Muñoz-Sabater, J., Nicolas, J.,
517 Peubey, C., Radu, R., Schepers, D., Simmons, A., Soci, C., Abdalla, S., Abellán, X., Balsamo,
518 G., Bechtold, P., Biavati, G., Bidlot, J., Bonavita, M., Chiara, G., Dahlgren, P., Dee, D.,
519 Diamantakis, M., Dragani, R., Flemming, J., Forbes, R., Fuentes, M., Geer, A., Haimberger, L.,
520 Healy, S., Hogan, R. J., Hólm, E., Janisková, M., Keeley, S., Laloyaux, P., Lopez, P., Lupu, C.,
521 Radnoti, G., Rosnay, P., Rozum, I., Vamborg, F., Villaume, S., and Thépaut, J.: The ERA5
522 global reanalysis, *Q.J.R. Meteorol. Soc.*, 146, 1999–2049, <https://doi.org/10.1002/qj.3803>, 2020.

523

524 Hiederer, R.: Mapping soil properties for Europe: spatial representation of soil database
525 attributes., Publications Office, LU, 2013.

526

527 Hrachowitz, M., Savenije, H. H. G., Blöschl, G., McDonnell, J. J., Sivapalan, M., Pomeroy, J. W.,
528 Arheimer, B., Blume, T., Clark, M. P., Ehret, U., Fenicia, F., Freer, J. E., Gelfan, A., Gupta, H.
529 V., Hughes, D. A., Hut, R. W., Montanari, A., Pande, S., Tetzlaff, D., Troch, P. A., Uhlenbrook,
530 S., Wagener, T., Winsemius, H. C., Woods, R. A., Zehe, E., and Cudennec, C.: A decade of
531 Predictions in Ungauged Basins (PUB)—a review, *Hydrological Sciences Journal*, 58, 1198–
532 1255, <https://doi.org/10.1080/02626667.2013.803183>, 2013.

533

534 Javelle, P., Fouchier, C., Arnaud, P., and Lavabre, J.: Flash flood warning at ungauged
535 locations using radar rainfall and antecedent soil moisture estimations, *Journal of Hydrology*,
536 394, 267–274, <https://doi.org/10.1016/j.jhydrol.2010.03.032>, 2010.

537

538 Jolliffe, I. T. and Stephenson, D. B. (Eds.): *Forecast Verification: A Practitioner's Guide in*
539 *Atmospheric Science*, John Wiley & Sons, Ltd, Chichester, UK,
540 <https://doi.org/10.1002/9781119960003>, 2011.

541

542 Li, J., Wang, Z., Wu, X., Xu, C.-Y., Guo, S., and Chen, X.: Toward Monitoring Short-Term
543 Droughts Using a Novel Daily Scale, Standardized Antecedent Precipitation Evapotranspiration
544 Index, 21, 891–908, <https://doi.org/10.1175/JHM-D-19-0298.1>, 2020.

545

546 Loh, W. Y. and Shih, Y. S.: Split Selection Methods for Classification Trees, 7, 815–840, 1997.
547 Martínez-Fernández, J., González-Zamora, A., Sánchez, N., and Gumuzzio, A.: A soil water
548 based index as a suitable agricultural drought indicator, *Journal of Hydrology*, 522, 265–273,
549 <https://doi.org/10.1016/j.jhydrol.2014.12.051>, 2015.

550

551 Martínez-Fernández, J., González-Zamora, A., Sánchez, N., Gumuzzio, A., and Herrero-
552 Jiménez, C. M.: Satellite soil moisture for agricultural drought monitoring: Assessment of the
553 SMOS derived Soil Water Deficit Index, *Remote Sensing of Environment*, 177, 277–286,
554 <https://doi.org/10.1016/j.rse.2016.02.064>, 2016.

555

556 Ma, K., Feng, D., Lawson, K., Tsai, W.-P., Liang, C., Huang, X., Sharma, A., Shen, C.:
557 Transferring hydrologic data across continents – leveraging data-rich regions to improve
558 hydrologic prediction in data-sparse regions. *Water Resources Research*, 57, e2020WR028600.
559 <https://doi.org/10.1029/2020WR028600>, 2021.

560

561 Massari, C., Modanesi, S., Dari, J., Gruber, A., De Lannoy, G. J. M., Girotto, M., Quintana-
562 Seguí, P., Le Page, M., Jarlan, L., Zribi, M., Ouaadi, N., Vreugdenhil, M., Zappa, L., Dorigo, W.,
563 Wagner, W., Brombacher, J., Pelgrum, H., Jaquot, P., Freeman, V., Volden, E., Fernandez
564 Prieto, D., Tarpanelli, A., Barbetta, S., and Brocca, L.: A Review of Irrigation Information
565 Retrievals from Space and Their Utility for Users, *Remote Sensing*, 13, 4112,
566 <https://doi.org/10.3390/rs13204112>, 2021.

567

568 Masson, V., Le Moigne, P., Martin, E., Faroux, S., Alias, A., Alkama, R., Belamari, S., Barbu, A.,
569 Boone, A., Bouyssel, F., Brousseau, P., Brun, E., Calvet, J. C., Carrer, D., Decharme, B., Delire,
570 C., Donier, S., Essaouini, K., Gibelin, A. L., ... Voldoire, A. (2013). The SURFEXv7.2 land and
571 ocean surface platform for coupled or offline simulation of earth surface variables and fluxes.
572 *Geoscientific Model Development*, 6(4), 929–960. <https://doi.org/10.5194/gmd-6-929-2013>

573

574 McKay, M. D., Beckman, R. J., and Conover, W. J.: Comparison of Three Methods for Selecting
575 Values of Input Variables in the Analysis of Output from a Computer Code, *Technometrics*, 21,
576 239–245, <https://doi.org/10.1080/00401706.1979.10489755>, 1979.

577

578 Merlin, O., Escorihuela, M. J., Mayoral, M. A., Hagolle, O., Al Bitar, A., and Kerr, Y.: Self-
579 calibrated evaporation-based disaggregation of SMOS soil moisture: An evaluation study at 3
580 km and 100 m resolution in Catalonia, Spain, *Remote Sensing of Environment*, 130, 25–38,
581 <https://doi.org/10.1016/j.rse.2012.11.008>, 2013.

582

583 Mishra, A., Vu, T., Veettil, A. V., and Entekhabi, D.: Drought monitoring with soil moisture active

584 passive (SMAP) measurements, *Journal of Hydrology*, 552, 620–632,
585 <https://doi.org/10.1016/j.jhydrol.2017.07.033>, 2017.

586

587 Muñoz Sabater, J.: ERA5-Land hourly data from 1981 to present. Copernicus Climate Change
588 Service (C3S) Climate Data Store (CDS), 10.24381/cds.e2161bac, 2020.

589

590 Noguera, I., Domínguez-Castro, F., and Vicente-Serrano, S. M.: Flash Drought Response to
591 Precipitation and Atmospheric Evaporative Demand in Spain, *Atmosphere*, 12, 165,
592 <https://doi.org/10.3390/atmos12020165>, 2021.

593

594 Noilhan, J. and Mahfouf, J.-F.: The ISBA land surface parameterisation scheme, *Global and*
595 *Planetary Change*, 13, 145–159, [https://doi.org/10.1016/0921-8181\(95\)00043-7](https://doi.org/10.1016/0921-8181(95)00043-7), 1996.

596

597 Panagos, P., Van Liedekerke, M., Jones, A., and Montanarella, L.: European Soil Data Centre:
598 Response to European policy support and public data requirements, *Land Use Policy*, 29, 329–
599 338, <https://doi.org/10.1016/j.landusepol.2011.07.003>, 2012.

600

601 Pena-Gallardo, M., Vicente-Serrano, S. M., Domínguez-Castro, F., and Beguería, S.: The
602 impact of drought on the productivity of two rainfed crops in Spain, *Nat. Hazards Earth Syst.*
603 *Sci.*, 19, 1215–1234, <https://doi.org/10.5194/nhess-19-1215-2019>, 2019.

604

605 Perrin, C., Michel, C., and Andréassian, V.: Improvement of a parsimonious model for
606 streamflow simulation, *Journal of Hydrology*, 279, 275–289, [https://doi.org/10.1016/S0022-1694\(03\)00225-7](https://doi.org/10.1016/S0022-1694(03)00225-7), 2003.

608

609 Piedallu, C., Gégout, J.-C., Perez, V., and Lebougeois, F.: Soil water balance performs better
610 than climatic water variables in tree species distribution modelling: Soil water balance improves
611 tree species distribution models, *Global Ecology and Biogeography*, 22, 470–482,
612 <https://doi.org/10.1111/geb.12012>, 2013.

613

614 Quintana-Seguí, P., Le Moigne, P., Durand, Y., Martin, E., Habets, F., Baillon, M., Canellas, C.,
615 Franchisteguy, L., and Morel, S.: Analysis of Near-Surface Atmospheric Variables: Validation of
616 the SAFRAN Analysis over France, 47, 92–107, <https://doi.org/10.1175/2007JAMC1636.1>,
617 2008.

618

619 Quintana-Seguí, P., Turco, M., Herrera, S., and Miguez-Macho, G.: Validation of a new
620 SAFRAN-based gridded precipitation product for Spain and comparisons to Spain02 and ERA-
621 Interim, *Hydrol. Earth Syst. Sci.*, 21, 2187–2201, <https://doi.org/10.5194/hess-21-2187-2017>,
622 2017.

623

624 Quintana-Seguí, P., Barela-Ortiz, A., Regueiro-Sanfiz, S., and Miguez-Macho, G.: The Utility of
625 Land-Surface Model Simulations to Provide Drought Information in a Water Management
626 Context Using Global and Local Forcing Datasets, *Water Resour Manage*,
627 <https://doi.org/10.1007/s11269-018-2160-9>, 2019.

628

629 Raymond, F., Ullmann, A., Tramblay, Y., Drobinski, P., and Camberlin, P.: Evolution of
630 Mediterranean extreme dry spells during the wet season under climate change, *Reg Environ*
631 *Change*, 19, 2339–2351, <https://doi.org/10.1007/s10113-019-01526-3>, 2019.

632

633 Reynolds, C. A., Jackson, T. J., and Rawls, W. J.: Estimating soil water-holding capacities by

634 linking the Food and Agriculture Organization Soil map of the world with global pedon
635 databases and continuous pedotransfer functions, *Water Resour. Res.*, 36, 3653–3662,
636 <https://doi.org/10.1029/2000WR900130>, 2000.

637

638 Rodell, M., Houser, P. R., Jambor, U., Gottschalck, J., Mitchell, K., Meng, C.-J., Arsenault, K.,
639 Cosgrove, B., Radakovich, J., Bosilovich, M., Entin, J. K., Walker, J. P., Lohmann, D., and Toll,
640 D.: The Global Land Data Assimilation System, *Bull. Amer. Meteor. Soc.*, 85, 381–394,
641 <https://doi.org/10.1175/BAMS-85-3-381>, 2004.

642

643 Stefan, V.G., Indrio G., Escorihuela M.J., Quintana-Seguí P., and Villar, J.M.: High-Resolution
644 SMAP-Derived Root-Zone Soil Moisture Using an Exponential Filter Model Calibrated per Land
645 Cover Type, *Remote Sensing* [2024](https://doi.org/10.3390/rs13061112), 13(6). <https://doi.org/10.3390/rs13061112>, [2021](https://doi.org/10.3390/rs13061112).

646

647 Stein, L., Clark, M. P., Knoben, W. J. M., Pianosi, F., and Woods, R. A.: How Do Climate and
648 Catchment Attributes Influence Flood Generating Processes? A Large-Sample Study for 671
649 Catchments Across the Contiguous USA, *Water Res.*, 57,
650 <https://doi.org/10.1029/2020WR028300>, 2021.

651

652 Tramblay, Y., Bouaicha, R., Brocca, L., Dorigo, W., Bouvier, C., Camici, S., and Servat, E.:
653 Estimation of antecedent wetness conditions for flood modelling in northern Morocco, *Hydrol.*
654 *Earth Syst. Sci.*, 16, 4375–4386, <https://doi.org/10.5194/hess-16-4375-2012>, 2012.

655

656 Tramblay, Y., Amoussou, E., Dorigo, W., and Mahé, G.: Flood risk under future climate in data
657 sparse regions: Linking extreme value models and flood generating processes, *Journal of*
658 *Hydrology*, 519, 549–558, <https://doi.org/10.1016/j.jhydrol.2014.07.052>, 2014.

659

660 Tramblay, Y., Koutoulis, A., Samaniego, L., Vicente-Serrano, S. M., Volaire, F., Boone, A., Le
661 Page, M., Llasat, M. C., Albergel, C., Burak, S., Cailleret, M., Kalin, K. C., Davi, H., Dupuy, J.-L.,
662 Greve, P., Grillakis, M., Hanich, L., Jarlan, L., Martin-StPaul, N., Martínez-Vilalta, J., Mouillot, F.,
663 Pulido-Velazquez, D., Quintana-Seguí, P., Renard, D., Turco, M., Türkeş, M., Trigo, R., Vidal,
664 J.-P., Vilagrosa, A., Zribi, M., and Polcher, J.: Challenges for drought assessment in the
665 Mediterranean region under future climate scenarios, *Earth-Science Reviews*, 210, 103348,
666 <https://doi.org/10.1016/j.earscirev.2020.103348>, 2020.

667

668 Tyralis, H., Papacharalampous, G., and Langousis, A.: A Brief Review of Random Forests for
669 Water Scientists and Practitioners and Their Recent History in Water Resources, *Water*, 11,
670 910, <https://doi.org/10.3390/w11050910>, 2019.

671

672 Vicente-Serrano, S. M., Lopez-Moreno, J.-I., Beguería, S., Lorenzo-Lacruz, J., Sanchez-
673 Lorenzo, A., García-Ruiz, J. M., Azorin-Molina, C., Morán-Tejeda, E., Revuelto, J., Trigo, R.,
674 Coelho, F., and Espejo, F.: Evidence of increasing drought severity caused by temperature rise
675 in southern Europe, *Environ. Res. Lett.*, 9, 044001, <https://doi.org/10.1088/1748-9326/9/4/044001>, 2014.

677

678 Willgoose, G. and Perera, H.: A simple model of saturation excess runoff generation based on
679 geomorphology, steady state soil moisture, *Water Resour. Res.*, 37, 147–155,
680 <https://doi.org/10.1029/2000WR900265>, 2001.

681

682 Wösten, J. H. M., Lilly, A., Nemes, A., and Le Bas, C.: Development and use of a database of
683 hydraulic properties of European soils, *Geoderma*, 90, 169–185, <https://doi.org/10.1016/S0016>

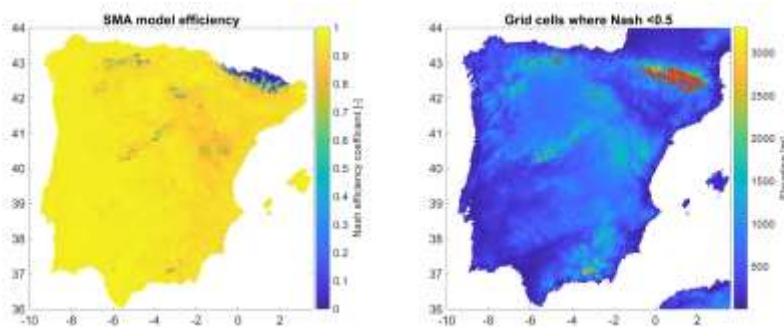
684 7061(98)00132-3, 1999.
685
686 Zhao, B., Dai, Q., Han, D., Dai, H., Mao, J., Zhuo, L., and Rong, G.: Estimation of soil moisture
687 using modified antecedent precipitation index with application in landslide predictions,
688 Landslides, 16, 2381–2393, <https://doi.org/10.1007/s10346-019-01255-y>, 2019.
689
690
691
692
693
694
695
696
697

698 **TABLE**

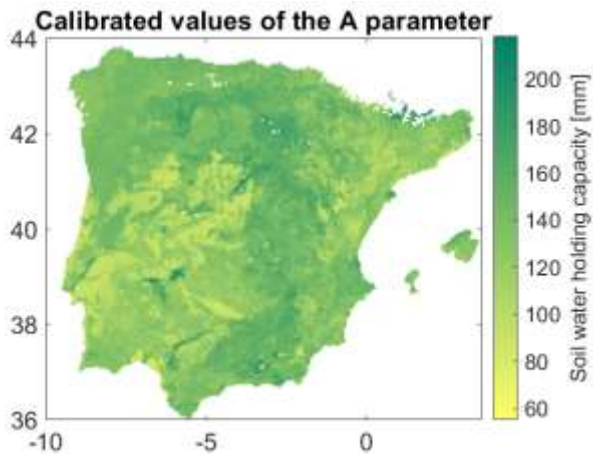
699
700 Table 1: Contingency table of the comparison between forecasts and observations or
701 any two analyses. The symbols a–d are the different numbers of cases observed to
702 occur in each category.
703

		Observations	
Forecast		1	0
1		a (hit)	b (false alarm)
0		c (miss)	d (correct rejection)

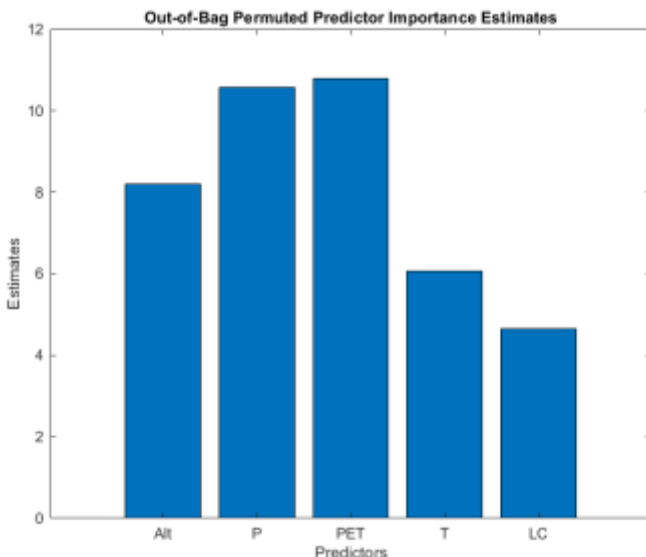
704
705 **FIGURES**
706
707



708
709 Figure 1: Efficiency of the SMA model to reproduce soil moisture from SURFEX
710
711
712

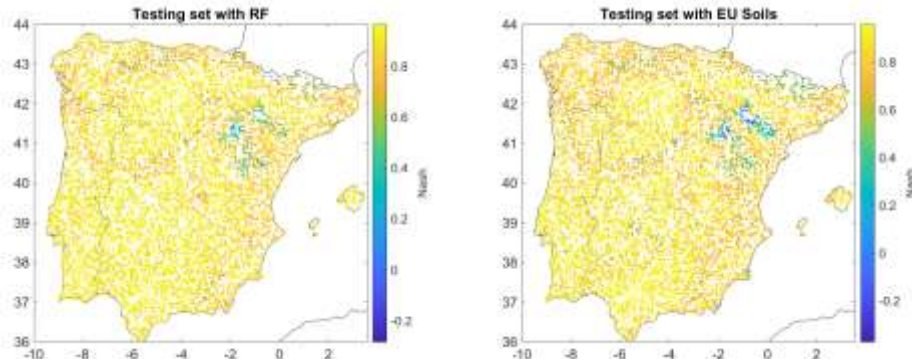


713
714 Figure 2: Map of the calibrated values of the A parameter of the SMA model
715
716

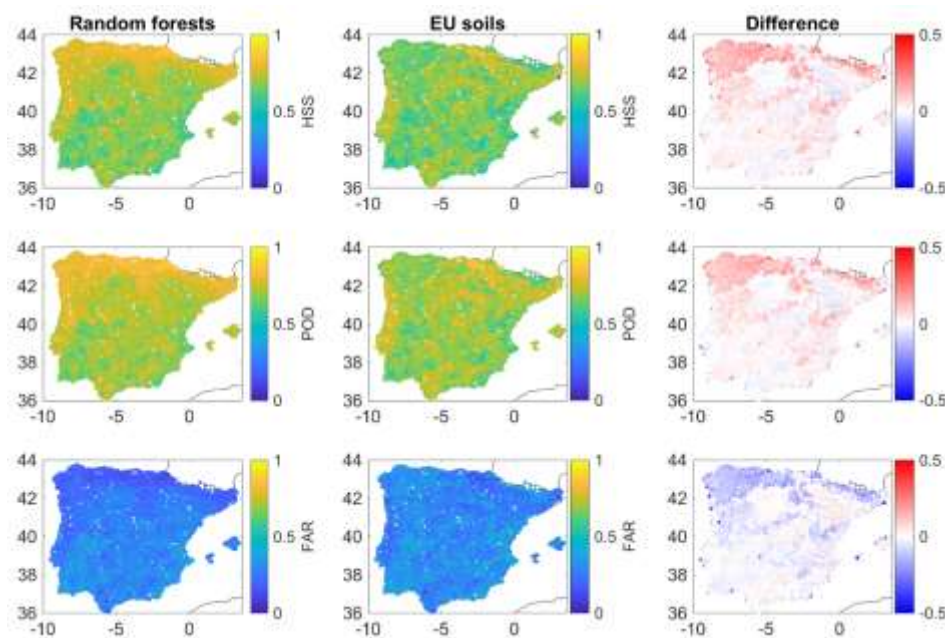


717
718 Figure 3: Relative importance of each predictor (Alt= altitude, P= precipitation, PET=
719 potential evapotranspiration, T=temperature, LC=land cover classes) in the Random
720 Forest method
721

722
723

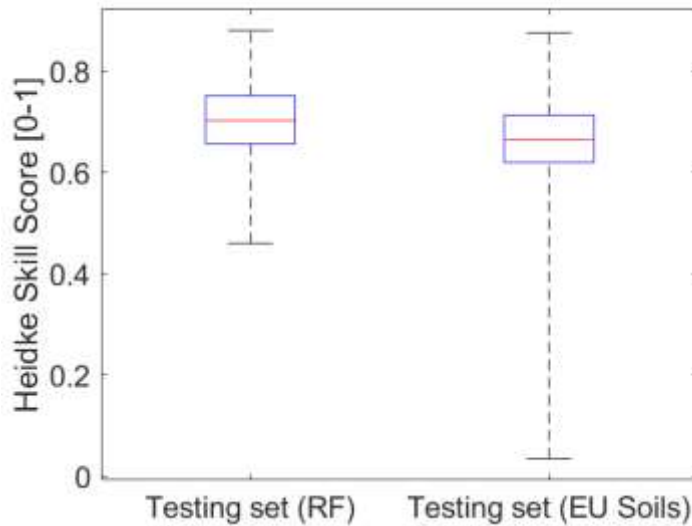


724
725 Figure 4: Nash efficiency coefficient obtained for the testing set, with the A parameter of
726 the SMA model estimated by RF (left) or ESDB (right)
727
728



729
730
731 Figure 5: Validation results in terms of HSS, POD and FAR with A estimated with either
732 Random Forests or European soil database.

733
734
735



736
737 Figure 6: Boxplot of the HSS obtained with RF or EU soil maps. The limits of the box
738 represent the 25th and 75 percentiles, the line in the middle refers to the median, and
739 the limits of the whiskers extend to the minimum and maximum values.
740
741
742
743
744
745
746
747